Biosensors and Bioelectronics 74 (2015) 384–390

Contents lists available at ScienceDirect

Biosensors and Bioelectronics

journal homepage: www.elsevier.com/locate/bios

Feasible electrochemical biosensor based on plasma polymerization-assisted composite of polyacrylic acid and hollow TiO_2 spheres for sensitively detecting lysozyme

Zhihong Zhang [a,b,*], Shuai Zhang [b], Linghao He [b], Donglai Peng [b], Fufeng Yan [b], Minghua Wang [a], Jihong Zhao [a], Hongzhong Zhang [a], Shaoming Fang [a,b,*]

[a] Henan Collaborative Innovation Center of Environmental Pollution Control and Ecological Restoration, Zhengzhou University of Light Industry, Zhengzhou, PR China

[b] State Laboratory of Surface and Interface Science of Henan Province Zhengzhou University of Light Industry, No. 166, Science Avenue, Zhengzhou 450001, PR China

ARTICLE INFO

Article history:
Received 9 April 2015
Received in revised form
15 June 2015
Accepted 25 June 2015
Available online 2 July 2015

Keywords:
Plasma polymerized acrylic acid
Hollow TiO_2 spheres
Electrochemical biosensor
Lysozyme detection

ABSTRACT

A composite made of polyacrylic acid and hollow TiO_2 spheres (TiO_2@PPAA) was prepared by the plasma polymerization method and subsequently used as an electrode material for detecting lysozyme. The chemical structure, surface morphology, and electrochemical performance of the TiO_2@PPAA composite were mainly affected by the plasma input power used during plasma polymerization. After optimizing plasma conditions, aptamer strands exhibited high adsorption affinity toward the surface of TiO_2@PPAA composite via synergistic effects between TiO_2 and PPAA. Electrochemical impedance spectroscopy results showed that the developed TiO_2@PPAA aptasensor presents highly sensitive detection ability toward lysozyme; the limit of detection of the proposed aptasensor is 0.015 ng mL^{-1} (1.04 pM) within the range of 0.05–100 ng mL^{-1} in terms of 3σ value. The film further showed excellent selectivity toward lysozyme in the presence of interfering proteins, such as thrombin, bovine serum albumin, and immunoglobulin E. Thus, this aptasensing strategy might broaden the applications of plasma polymerized nanomaterials in the field of biomedical research and early clinical diagnosis.

1. Introduction

Lysozyme, also as muramidase or peptidoglycan *N*-acetylmuramoyl-hydrolase, is a small spheroidal hydrolase responsible for breaking down the polysaccharide walls of Gram-positive bacteria and certain Gram-negative bacteria (Wang et al., 2009). Eggwhites, which contain approximately 3.5% lysozyme, are a main lysozyme source. As such, hen eggwhite lysozyme has long been used as a prominent model system for systematic studies on protein–protein interactions and development of new detection methods. Lysozyme is ubiquitous in cells, and changes in its level in serum and urine could be indicative of many diseases such as cancer, HIV, and myeloid leukemia (Wang et al., 2010). Owing to the physiological importance of lysozymes, developing new, rapid, inexpensive and effective biosensors for their detection has been given considerable significance (Guo et al., 2007).

A number of aptasensors have recently been reported for lysozyme detection through various signal read-out assays, including electrochemistry (Rodríguez and Rivas, 2009), piezoelectricity (Mao et al., 2001), quartz crystal microbalance (QCM) (Sener et al., 2010), colorimetry, fluorescence (Song et al., 2014), and surface-enhanced Raman scattering (SERS) (Li et al., 2012) Assays. Among these sensors, electrochemical aptasensors have been reported for lysozyme detection and thus attracted increased research interest (Mihai et al., 2015). As an electrochemical approach, electrochemical impedance spectroscopy (EIS) is reliable, sensitive, and compatible with DNA biochips. This technique has become one of the most promising methods for probing the features of surface-modified electrodes (Keighley et al., 2008). Compared with routine determination approaches, electrochemical measurements offer short analytical times, high sensitivity, and a wide range of applications (Labib and Berezovski, 2014). Normally, the electrode is modified by nanomaterials (Wang, 2005), polymeric films (Heineman et al., 1980), or self-assembled layers (Yang et al., 2006) to

* Corresponding authors at: State Laboratory of Surface and Interface Science of Henan Province Zhengzhou University of Light Industry, No. 166, Science Avenue, Zhengzhou 450001, PR China.

E-mail addresses: mainzhh@163.com (Z. Zhang), mingfang@zzuli.edu.cn (S. Fang).

http://dx.doi.org/10.1016/j.bios.2015.06.062
0956-5663/

enhance the electrochemical signal for sensitively detecting the target molecules.

Among the polymeric films currently available, plasma-polymerized nanofilms exhibit unique properties, being pinhole-free, highly cross-linking, amorphous, all-dry, adhesive, and highly resistant to chemical and physical treatments on most substrates (Ricciardi et al., 2012; Rivolo et al., 2014). Plasma polymerization is typically a clean process that allows production of a thin functional polymeric film by selection of proper monomers (Garcia-Torres et al., 2014); the resultant films could be used as coatings (Da Silva Sobrinho et al., 1998) or biocompatible layers (Losic et al., 2008). Functional plasma polymeric films containing amino groups (–NH_2) (He et al., 2012), carboxyl groups (–COOH) (He et al., 2012), and hydroxyl groups (–OH) (Garcia et al., 2009) are usually utilized as organic precursors and matrices for protein and DNA biosensors. Additionally, plasma polymerized nanofilm was used to adsorb lysozyme (Hirotsu and Tagaki, 2004; Messina et al., 2009). However, there is no report about the detection of lysozyme using the plasma polymerized surface as the sensitive layer.

Given that small unsaturated monomer molecules are decomposed into various species by plasma irradiation, the plasma polymer chain shows poor regularity. Even for monomers that could be polymerized into conductive polymers, such as pyrrole, aniline, or thiophene, the related plasma polymerized nanofilms are often devoid of electrochemical performance. As a consequence, plasma polymers are rarely used as electrochemical biosensors. To overcome this shortcoming, enhancing the electrochemical performance of plasma polymer films via modification using nanomaterials is necessary.

TiO_2 spheres exhibit large surface areas and good functionality with hydroxyl groups (–OH) (Kanehira et al., 2008). This material has also been applied as a DNA separator because it provides a large surface/volume ratio and binds more biomolecules (Jeon et al., 2014). Recent studies have attempted to produce TiO_2 composite nanoscale materials through a variety of plasma-based techniques. TiO_2 nanoparticles have been coated with polyacrylic acid by plasma-enhanced chemical vapor deposition (PECVD) to explore the effects of the coating on the dispersion of treated nanoparticles in water (Solís-Gómez et al., 2014). The surfaces of PET/TiO_2 thin film have been modified by glow discharge plasma as a function of discharge potential for improving bioactivity (Pandiyaraj et al., 2010). Compared with TiO_2 nanoparticles, hollow TiO_2 spheres exhibit higher specific surface areas and catalytic activities (Liu et al., 2010). To the best of our knowledge, however, no report has yet investigated electrochemical DNA or aptamer biosensors based on nanocomposites composed of PPAA acid and hollow TiO_2 spheres.

In this work, a composite film composed of hollow TiO_2 spheres and PPAA (TiO_2@PPAA) was prepared by PECVD and used as an electrochemical biosensor for detecting lysozyme (Scheme 1). The electrochemical aptasensor developed exhibited high sensitivity toward lysozyme and selectivity toward other proteins. Compared with routine methods, the fabricated biosensor shows two advantages: (i) the presence of hollow TiO_2 spheres within TiO_2@PPAA composite enhances the electrochemical performance of the sensing layer and (ii) abundant carboxyl groups improve immobilization of more aptamer molecules and lowers the lysozyme limit of detection (LOD).

2. Experimental section

2.1. Chemicals and materials

Acrylic acid, *N*-hydroxysuccinimide (NHS), 1-ethyl-3-(3-dimethylaminopropyl) carbodiimide hydrochloride (EDC), *n*-butyl titanate, and anhydrous glucose were sourced from Aladdin (Shanghai, China). Aptamer (5′-NH_2-ATCAGGGCTAAAGAGTGCA-GAGTTACTTAG-3′); thrombin, lysozyme, human immunoglobulin E (IgE), and bovine serum albumin (BSA) were obtained from Beijing SBS Genetech Co., Ltd. (China). All other reagents used were of analytical grade and employed as received.

2.2. Modification of the gold electrode with hollow TiO_2 spheres

A gold electrode (diameter, 3 mm) (AE) was used as the working electrode for electrochemical measurement. AEs were polished with 0.05 mm alumina slurries, ultrasonically washed in

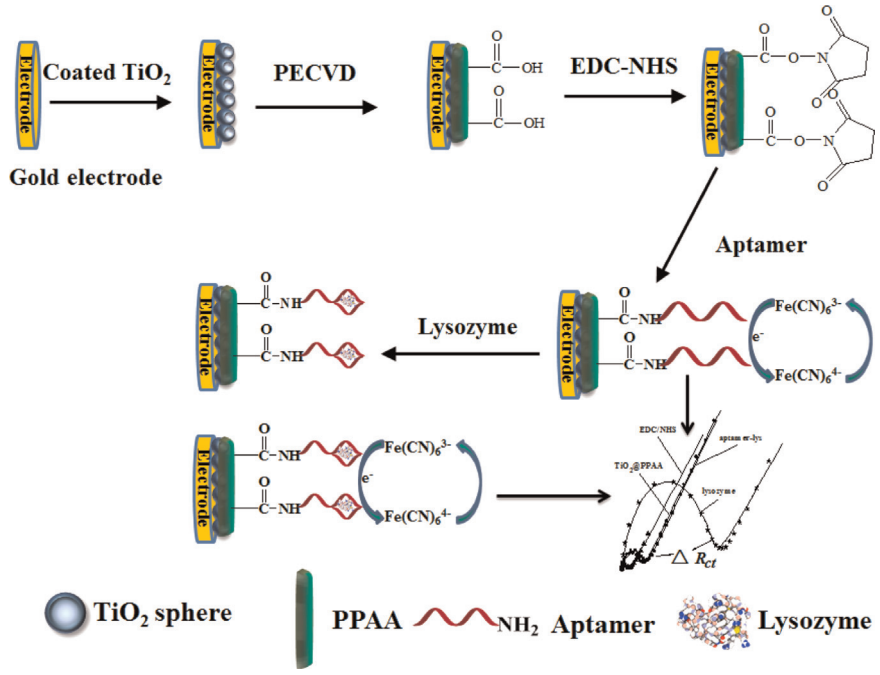

Scheme 1. Schematic representation of the electrochemical aptasensor based on TiO_2@PPAA composite for detecting lysozymes.

ultrapure water, and electrochemically cleaned through oxidation and reduction cycling in 0.5 M H_2SO_4 from −0.2 V to 1.6 V (versus Ag/AgCl).

The preparation of hollow TiO_2 spheres is presented in the Supporting information (Fig. S1a and b). Hollow TiO_2 spheres were dispersed in ethanol at a concentration of 1 mg mL^{-1}. 10 μL of TiO_2 spheres dispersion was dropped onto the AE surface and dried in air; this procedure was followed by further modification with PPAA in a plasma chamber.

2.3. Preparation of buffer, electrolyte, aptamer, and protein solutions

Aptamer, lysozyme, BSA, thrombin, and IgE solutions were prepared using phosphate buffer solution (PBS) (pH 7.4). This buffer solution was prepared by mixing 0.067 M Na_2HPO_4 and 0.067 M KH_2PO_4 in $\nu(Na_2HPO_4):\nu(KH_2PO_4)=(8:2)$. The electrolyte solution was prepared immediately before use by dissolving 1.65 g $K_3[Fe(CN)_6]$, 2.11 g $K_4[Fe(CN)_6]$, 8 g NaCl, and 0.2 g KCl in 1 L of PBS. All solutions were prepared immediately prior to the experiments and stored at 4 °C until use. The lysozyme stock solution was dissolved in PBS at a concentration of 1 mg mL^{-1}.

2.4. Preparation of PPAA and TiO_2@PPAA composite

Plasma modification was performed in a HQ-2 PECVD system manufactured by the Institute of Microelectronics of the Chinese Academy of Sciences, China. The radio frequency generator was operated at 13.56 MHz. PPAA film was deposited onto AEs modified with hollow TiO_2 spheres under plasma input powers of 20, 50, or 100 W for various periods of time at a continuous wave; here, acrylic acid was used as the monomer. The gas flow rate was fixed at 10 sccm, and the pressure was kept constant at 0.1 Pa. After the TiO_2@PPAA composite had been deposited onto the pretreated AE (AE–TiO_2@PPAA) (Fig. S1c and d), therefore, the resulting material was immersed in PBS solution overnight to remove any unbound monomer molecules or oligomers in the polymeric network (Van Os et al., 1998; Wang et al., 2004; Zhang et al., 2003).

2.5. Fabrication of the electrochemical aptasensor based on TiO_2@PPAA composite

AE–TiO_2@PPAA was immersed in 10 mL of PBS (pH 7.4) containing a mixture of 1 mM NHS and 4 mM EDC at 4 °C for 2 h. In this system, the carboxyl groups of TiO_2@PPAA could be activated into active ester groups (Guo et al., 2004). Afterward, the material was washed with Milli-Q water and then dried under a N_2 stream. Subsequently, the TiO_2@PPAA composite was incubated in a solution of 200 nM aptamer for 2 h. Once the aptamer had been anchored to the TiO_2@PPAA composite, the resulting electrode was employed as an aptasensor to detect lysozymes. Various concentrations of lysozyme solution were circulated into the system to determine the detection limit of the sensor toward the analyte. The specificity of the aptasensor was determined by incubation with thrombin, BSA, and IgE for 2 h. To demonstrate the potential of the aptasensor for lysozyme analysis in eggwhite, the aptasensor was incubated in different eggwhite concentrations.

2.6. Characterizations

Chemical structures and components were analyzed by X-ray photoelectron spectroscopy (XPS) using a VG ESCALAB HP photoelectron spectrometer equipped with an analyzer and preparation chambers. An Al Kα ($h\nu=1486.6$ eV) X-ray source with a power ≤ 100 W was used to record the spectra. A silicon wafer was used as the substrate for XPS characterization. Surface morphology was analyzed with SEM (JSM-6490LV, Japan, operated at 20 kV). The sample was cleaned using piranha solution (70% H_2SO_4/30% H_2O_2), followed by washing with Milli-Q H_2O for several times. Fourier-transform infrared (FT-IR) spectra were obtained by deposition of PPAA on KBr pellets coated with TiO_2. Each FT-IR spectrum was collected by cumulating 32 scans at a resolution of 4 cm^{-1} from 400 to 4000 cm^{-1}. The thickness of plasma-polymerized films and composite was determined by a step profiler (Alpha Step IQ of KLA Tencor Co. Ltd.). To reduce the experimental deviations of the electrochemical measurements, the thicknesses of the pristine PPAA layer and TiO_2@PPAA composite deposited onto the substrates were kept consistent approximately, i.e., 54 ± 3 and 800 ± 25 nm, respectively.

2.7. Electrochemical measurements

EIS was performed using a CHI660D electrochemical workstation (Shanghai CH Instrument Company, Shanghai, China). All electrochemical measurements were performed via a conventional three-electrode system composed of AE, a Pt-slide auxiliary electrode, and an Ag/AgCl reference electrode in a 1:1 mixture of 5 mM $K_3[Fe(CN)_6]/K_4[Fe(CN)_6]$, 0.14 M NaCl, and 2 mM KCl. A frequency range of 1 mHz to 1 MHz was used. EIS spectra were analyzed using Zview2 software, which was described in the Supporting information (Fig. S5). Lysozyme concentrations were quantified by a decrease in electron transfer resistance ΔR_{ct} ($\Delta R_{ct}=R_{ct,0}-R_{ct,i}$), where $R_{ct,0}$ is the electron transfer resistance in the absence of lysozyme, and $R_{ct,i}$ is the electron transfer resistance in the presence of lysozyme (Sundfors et al., 2002). All electrochemical experiments were carried out at room temperature (25 ± 1 °C). Three parallel experiments were carried out for each measurement, their average values were applied in the present work.

3. Results and discussion

3.1. Chemical structure and components of TiO_2@PPAA composites

The chemical structure of the TiO_2@PPAA composite was mainly affected by the plasma conditions, such as plasma input power, plasma irradiation time, or pulse plasma duty cycles. The FT-IR spectra of TiO_2@PPAA composite prepared under plasma input powers of 20, 50, and 100 W are summarized in Fig. S2a. The visibly higher baseline of the spectrum from ~3450 cm^{-1} to ~3400 cm^{-1} suggests that the stretching vibrations of the –OH groups of TiO_2 spheres could be hidden in this range. Weak multiple adsorption bands at ~2900 and ~2970 cm^{-1} are attributed to CH_x bond stretching of the PPAA film (Hirotsu et al., 2002). The band at ~1450 cm^{-1} is attributed to the bending vibrations of –CH_2 groups (Ward et al., 2003), and the band at ~1720 cm^{-1} indicates the presence of –COOH groups (C=O stretching band) in the TiO_2@PPAA composite (Sciarratta et al., 2003). The adsorption bands at ~1050 and 1170–1190 cm^{-1} could be assigned to C–O stretching bands (Ward et al., 2003). The weak signals (~1630 cm^{-1}) may originate from C=C stretching of the acrylic acid monomer, which suggests that several monomer molecules remain in the composite composite. These results demonstrate that the FT-IR spectrum of the acrylic acid monomer varies from that of the developed composite (Fig. S2b). The peak density of the –COOH group (~1720 cm^{-1}) decreases along with increasing plasma input power, which is in agreement with a previous work (Zhang et al., 2014a). –COOH functional groups can be readily decomposed into smaller species by high plasma input power irradiation (Zhang et al., 2014a). The densities of –COOH in TiO_2@PPAA composite deposited under 20 and 50 W were

extremely close.

XPS determination of the TiO_2@PPAA composite deposited under different plasma input powers was conducted to investigate the detailed chemical components of the composite. XPS survey results show two elements of C 1*s* and O 1*s* (Fig. S3). The atomic percentages of C 1*s* and O 1*s* in the TiO_2@PPAA composite deposited at various plasma input powers are summarized in Table S1. This table shows that the C percentage increases from 63.9% to 77.5% with increasing plasma input power; this change may be due to the degree of fragmentation and rearrangement of the monomer (Fahmy et al., 2011). The C 1*s* core-level XPS spectra of TiO_2@PPAA composite deposited at 20, 50, and 100 W are shown in Fig. S4a. It mainly contains four components, corresponding to different chemical environments present in the composite. The peak at ~284.6 eV, is assigned to CH_x/C–C/C=C groups in the samples. Separating solely the peak of C=C is difficult because of its low intensity. The peak at ~285.9 eV is due to C–O, while the peak at ~286.7 eV may be due to C=O groups. The peak at ~288.7 eV is attributed to –COO– (Sciarratta et al., 2003). The presence of C–O and C=O groups reveals that –COOH groups in the TiO_2@PPAA composite could be decomposed by plasma irradiation. In the plasma chamber, carbon-related species could react with oxygen species to form gas molecules that are removed from the surface of the composite films (Zhang et al., 2014a). The XPS results are in good agreement with the FT-IR findings, and the relative amount of –COO– in the composite decreased with increasing input powers or deposition times (Fig. S4a). Weak signals of the Ti 2*p* core-level were observed in the XPS spectra of all of the samples (Fig. 4b) at lower plasma input powers. As the detection limit of XPS instruments is usually less than 8–10 nm, the chemical components or structures of the interior regions of the film could not be measured (Briggs et al., 1979). Since hollow TiO_2 spheres were fully covered by the thick PPAA films, leading to the weak Ti 2*p* signals observed.

3.2. Electrochemical measurements

Biomolecule immobilization generally influences the basic performance of the sensing layer, the pH or ionic strength of the buffer solution, and the concentration of the probe molecules. Thus, investigating the optimal conditions of lysozyme detection based on the fabricated biosensor is necessary. To evaluate the efficiency of lysozyme detection using the developed electrochemical biosensor based on TiO_2@PPAA composite, AEs modified with different materials, such as pristine hollow TiO_2 spheres, PPAA, and the TiO_2@PPAA composite, were used as aptasensors for lysozyme detection through EIS measurements. EIS can provide further information on impedance changes in the electrode surface during the modification process and detection procedures.

3.2.1. Effects of the plasma input power on the lysozyme detection

Herein, the effect of composite performance on lysozyme detection is discussed and other influences of the buffer solution and measurement conditions are neglected. As shown in Fig. 1a and Fig. S6, the EIS spectra of each step of the lysozyme detection procedure were collected using electrochemical biosensors fabricated from AE–TiO_2@PPAA composite deposited under different input powers of 20, 50, and 100 W. The R_{ct} of the bare AE is 0.062 kΩ; after coating with TiO_2 spheres, the R_{ct} of the resultant AE–TiO_2 electrode deposited at 20 W increased to 0.227 kΩ (Fig. 1a). This finding could be explained by the relatively poor electrochemical activity of TiO_2, which results in slow electron transfer at the interface between the modified electrode and the electrolyte solution (Wang et al., 2014). The simulated R_{ct} of the AE–TiO_2@PPAA composite electrode further increased to 0.345 kΩ after PPAA deposition because of the insulation afforded by the plasma-polymerized layer (Pryce Lewis et al., 2000). After activation of TiO_2@PPAA by EDC–NHS, however, the R_{ct} of the AE–TiO_2@PPAA electrode decreased to 0.06 kΩ. When the –COOH group of PPAA is activated through formation of an NHS ester intermediate (Erdem et al., 2010), EDC–NHS presents a more complex cross-linking mechanism and functions as a catalyst (Kang et al., 2015) to facilitate electron transfer in the EDC–NHS cross-linked TiO_2@PPAA composite (Pauliukaite et al., 2010), hence leading to a decrease in R_{ct}. When the aptamer is immobilized onto the activated electrode, amide groups are formed between the amino-modified aptamer and the activated ester groups in TiO_2@PPAA. The results show that the R_{ct} of the composite electrode increases to 0.508 kΩ. The anchored aptamer chains bear negative charges on its phosphate backbone and exerts an electrostatic repulsive force on the negatively charged probe anions $[Fe(CN)_6]^{3-/4-}$. When the developed aptasensors were used to detect lysozyme, the R_{ct} continuously increased to 0.714 kΩ, which could be due to formation of a barrier by the associated bulky lysozyme molecules that effectively impedes electron transfer of $[Fe(CN)_6]^{3-/4-}$ in solution (Nwankire et al., 2015; Venkatesh et al., 2015). All composite electrode systems modified with TiO_2@PPAA composite deposited at 20, 50, or 100 W showed similar trends during the lysozyme detection procedure.

Variations in R_{ct} at each step of lysozyme detection are summarized in Fig. 1b. Among the samples studied, the R_{ct} of TiO_2@PPAA composite deposited at 20 W was the lowest, which indicates that the electrochemical activity of this composite is superior to those of the other composites. This result also shows

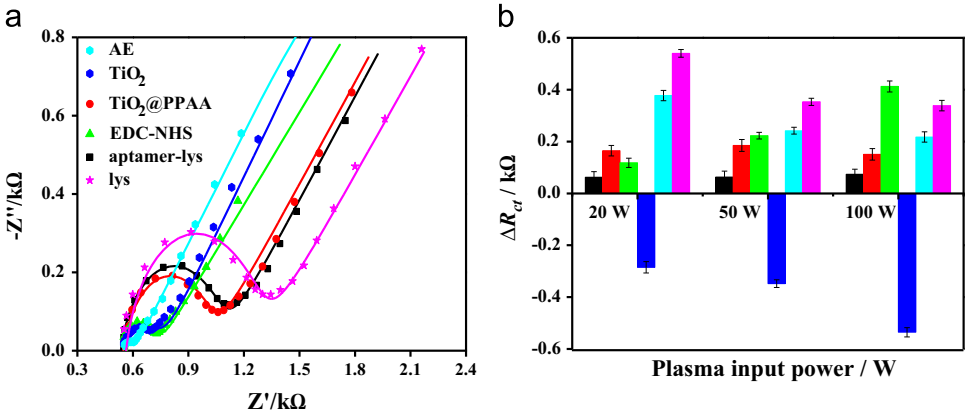

Fig. 1. EIS Nyquist plots of the lysozyme detection procedure using the fabricated electrochemical aptasensor based on a series of TiO_2@PPAA composite deposited under (a) 20 W for 3 min and (b) variations in R_{ct} at each stage of lysozyme detection based on the above samples and the R_{ct} of AE ( ), $R_{ct,\ TiO_2} - R_{ct,\ AE}$ ( ), $R_{ct,\ TiO_{2@PPAA}} - R_{ct,\ TiO_2}$ ( ), $R_{ct,\ EDC-NHS} - R_{ct,\ TiO_{2@PPAA}}$ ( ), $R_{ct,\ aptamer} - R_{ct,\ EDC-NHS}$ ( ), and $R_{ct,\ lys} - R_{ct,\ aptamer}$ ( ).

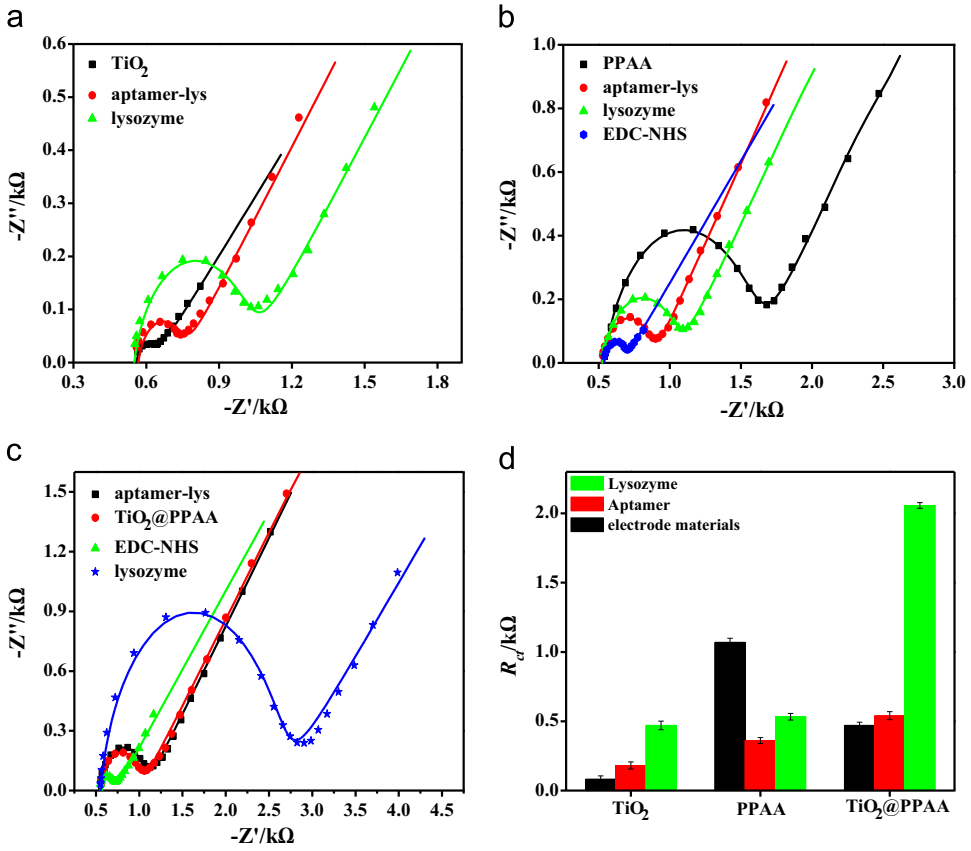

Fig. 2. EIS Nyquist plots of the developed electrochemical biosensor based on (a) pristine TiO_2 spheres, (b) as-prepared PPAA, and (c) TiO_2@PPAA composite deposited at 20 W for 3 min. (d) Variation in R_{ct} at each stage of lysozyme detection based on the above samples.

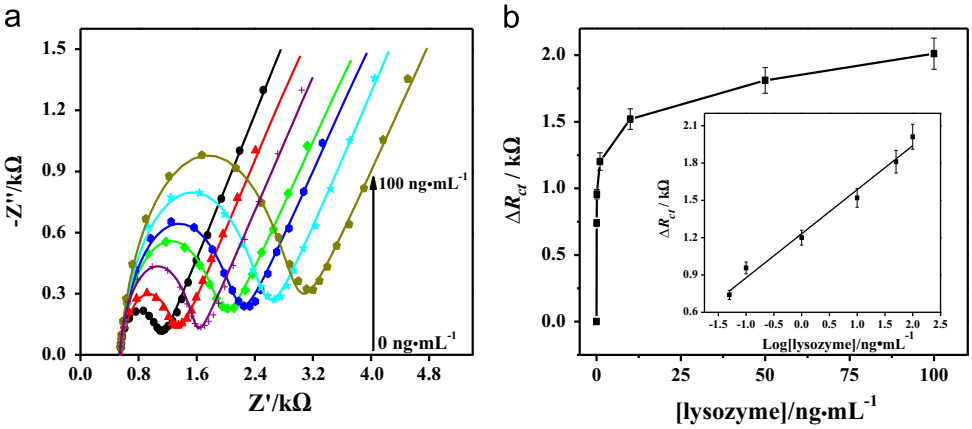

Fig. 3. (a) Nyquist plots of AE–TiO_2@PPAA composite after incubation with different concentrations of lysozyme ranging from 0 ng mL^{-1} to 100 ng mL^{-1}. (b) Dependence of (AE–TiO_2@PPAA) ΔR_{ct} on lysozyme concentration. Inset: ΔR_{ct} is linear with the logarithm of lysozyme concentrations ranging from 0.05 ng mL^{-1} to 100 ng mL^{-1}.

that aptamer molecules prefer to immobilize on the TiO_2@PPAA composite deposited under 20 W, thereby suggesting that the highest ΔR_{ct} may be obtained after aptamer anchoring. Other lysozyme molecules were subsequently determined using this electrochemical aptasensor. As discussed above, more carboxyl groups remain in the composite deposited under lower plasma input powers than in those deposited under higher plasma input powers. This finding indicates strong interactions between amino-group modified aptamer molecules. Hence, the TiO_2@PPAA composite prepared under 20 W for 3 min was used as the optimal film in succeeding experiments.

3.2.2. Comparison of the electrochemical performances of TiO_2, PPAA, and TiO_2@PPAA composite

To evaluate the modification efficiency of PPAA films by TiO_2 spheres, lysozyme detection using the electrochemical aptasensor based on hollow TiO_2 sphere-, PPAA-, and TiO_2@PPAA composite-modified electrodes are shown in Fig. 2a–c. The simulated R_{ct} of the composite electrode with pristine hollow TiO_2 spheres was approximately 0.21 kΩ, whereas that of the electrode modified with the as-prepared PPAA film was 1.07 kΩ. This finding indicates that the electrochemical activity of the PPAA film is weaker than that of TiO_2 spheres. Hence, the electrochemical performance of plasma polymeric films could be improved using inorganic nanoparticles, which leads to the intermediate R_{ct} of the TiO_2@PPAA composite (0.345 kΩ).

Table 1
LOD values of different materials for lysozyme detection.

Electrode of materials	Technique	Linear range	LOD	Reference
pcDNA-LBA	EIS	0.2 nM–4.0 nM	0.07 nM	Peng et al. (2009)
Chitosan–graphene oxide	EIS	0 nM–75 nM	28.53 nM	Erdem et al. (2014)
Multiwalled carbon nanotube	EIS	–	862 nM	Rohrbach et al. (2012)
TiO_2/three-dimensional reduced graphene oxide/PPy nanocomposite	DPV	0.007 nM–3.5 nM	5.5 pM	Wang et al. (2015)
Fe_2O_3 on graphene matrix	EIS	35 nM–35 mM	11.18 nM	Du et al. (2013)
TiO_2/PPAA	EIS	0.0035 nM–7 nM	1.04 pM	This work

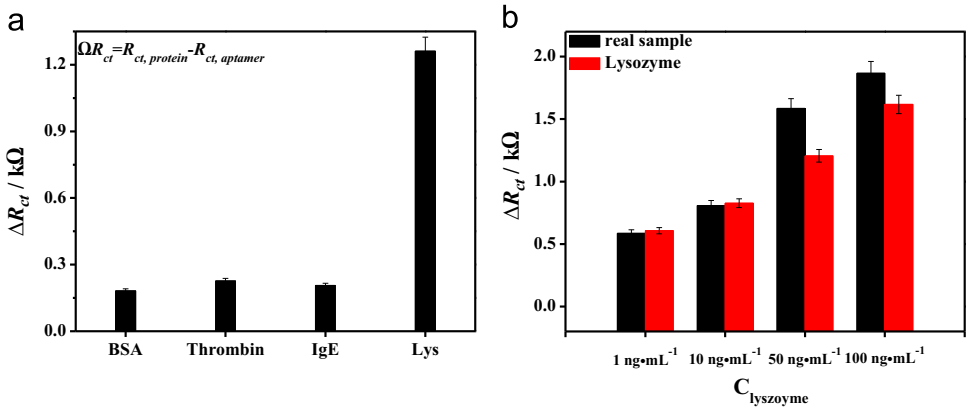

Fig. 4. (a) Detection of the ΔR_{ct} of 1 μg mL^{-1} BSA, 1 μg mL^{-1} thrombin, 1 μg mL^{-1} IgE, and 1 ng mL^{-1} lysozyme using the developed electrochemical biosensor based on TiO_2@PPAA deposited at 20 W for 3 min. (b) Nyquist plots of the AE–TiO_2@PPAA composite after reaction with comparison of the ΔR_{ct} of lysozyme and real samples.

Variations in R_{ct} at each step of the lysozyme detection procedure are summarized in Fig. 2d; here, the highest variation in R_{ct} before and after lysozyme detection was observed from the fabricated electrochemical aptasensor based on TiO_2@PPAA composite.

3.3. Sensitivity of lysozyme detection using the developed electrochemical biosensor

To assess the LOD and response range of the developed aptasensor for detecting lysozymes quantitatively, solutions with different lysozyme concentrations were incubated with the electrode. The image in Fig. 3a shows Nyquist plots of the responses of the electrode with AE–TiO_2@PPAA composite deposited at 20 W toward different lysozyme concentrations. Fig. 3b illustrates the dependence of ΔR_{ct} on lysozyme concentration (0.05–100 ng mL^{-1}). The inset in Fig. 3b shows that ΔR_{ct} is linear with the logarithm of lysozyme concentrations over the range of 0.05–100 ng mL^{-1}. The regression equation obtained is $\Delta R_{ct} = 1.232 + 0.354\ log\ C_{\ lysozyme}$ (unit of C, ng mL^{-1}), and the regression coefficient (R^2) is 0.982. The LOD was calculated in terms of the 3σ rule (Kaiser, 1973) and found to be 0.015 ng mL^{-1} (1.04 pM). The similar measurements of LOD toward the lysozyme detection using the different developed aptasensors, including AE–TiO_2@PPAA deposited at 50 (Fig. S7) and 100 W (Fig. S8), AE–TiO_2 (Fig. S9), and AE–PPAA (Fig. S10), were carried out and summarized in Table S2. The result shows that The LODs of lysozyme detection based on the electrochemical TiO_2@PPAA composite aptasensors were lower than those of analog aptasensors (Table 1).

3.4. Selectivity of the developed aptasensor

To confirm the specificity of the developed lysozyme aptasensor, control experiments were conducted using three proteins, namely, BSA, thrombin, and IgE. These proteins are also present in blood and exhibit properties similar to those of lysozyme; thus, these proteins may serve as interfering substances. Lysozyme strongly associates with proteins with low isoelectric points, and the isoelectric points of lysozyme, thrombin, BSA, and IgE are about 11, 7, 7.8, and 8.0, respectively (Iwamoto et al., 2012). Thus, these proteins are excellent samples to use during assessment of the specificity of the developed AE–TiO_2@PPAA for lysozyme. When BSA (1 μg–mL^{-1}), thrombin (1 μg mL^{-1}), IgE (1 μg mL^{-1}), and lysozyme (1 ng mL^{-1}) were incubated and detected individually by the aptasensor (Fig. 4a), only lysozyme induced significant ΔR_{ct} responses; the other proteins showed much lower responses. These results reveal that the three proteins do not interfere with lysozyme detection. Thus, the aptasensor has good selectivity for lysozyme.

3.5. Test of real samples

To investigate the actual performance of the developed biosensor, the lysozyme content in egg was examined. Eggs are composed of 3.5% lysozyme (Chen et al., 2011). The lysozyme in eggwhite sampled was diluted to 1, 10, 50, and 100 ng mL^{-1}. As shown in Fig. 4b, the eggwhite lysozyme solutions were then circulated for 2 h in the electrochemical measurement system with the AE–TiO_2@PPAA composite immobilized with the aptamer as the working electrode. Afterward, the composite electrode was thoroughly washed with 10 mM PBS (pH=7.0) to reduce nonspecific binding. At low concentrations of real samples, the R_{ct} of the real sample matched that of the lysozyme. When the real sample concentration exceeded 50 ng mL^{-1}, the ΔR_{ct} also exceeded that of the composite electrode immobilized with lysozyme. This result could be due to the interface of other proteins. In view of the properties of lysozymes in eggwhite, the results obtained may be considered satisfactory.

4. Conclusion

Plasma polymerization-assisted TiO_2@PPAA composite were fabricated and used as a sensing layer for lysozyme detection. The

intensity of carboxyl groups in the TiO_2@PPAA composite decreased with increasing plasma input power and irradiation time; this increase is closely linked to the adsorption affinity of the aptamer. Strong synergistic effects between PPAA and hollow TiO_2 led to films suitable for highly sensitive detection of lysozymes. The limit of lysozyme detection using the developed electrochemical aptasensor was calculated as 0.015 ng mL^{-1} (1.04 pM) within the range of 0.05–100 ng mL^{-1} in terms of 3σ value . Our results also showed minimal interferences from other proteins, i.e., BSA, IgE, and thrombin. Experimental results indicated that the aptasensor exhibits high sensitivity, selectivity, and applicability. All of these results demonstrate that TiO_2@PPAA composite could be used as promising electrochemical aptasensors.

Acknowledgment

This work was supported by program for the National Natural Science Foundation of China (NSFC: Account nos. 51173172 and 21104070) and Science and Technology Opening Cooperation Project of Henan Province (Account no. 132106000076).

Appendix A. Supplementary material

Supplementary data associated with this article can be found in the online version at http://dx.doi.org/10.1016/j.bios.2015.06.062.

References

Briggs, D., Brewis, D., Konieczko, M., 1979. J. Mater. Sci. 14 (6), 1344–1348.
Chen, Z., Li, L., Zhao, H., Guo, L., Mu, X., 2011. Talanta 83 (5), 1501–1506.
Da Silva Sobrinho, A., Latreche, M., Czeremuszkin, G., Klemberg-Sapieha, J., Wertheimer, M., 1998. J. Vac. Sci. Technol. A 16 (6), 3190–3198.
Du, M., Yang, T., Guo, X., Zhong, L., Jiao, K., 2013. Talanta 105 (15), 229–234.
Erdem, A., Eksin, E., Muti, M., 2014. Coll. Surf. B 115 (1), 205–211.
Erdem, A., Papakonstantinou, P., Murphy, H., McMullan, M., Karadeniz, H., Sharma, S., 2010. Electroanalysis 22 (6), 611–617.
Fahmy, A., Mix, R., Schönhals, A., Friedrich, J.F., 2011. Plasma Process. Polym. 8 (2), 147–159.
Garcia, C.G., Ferrus, L.L., Moratal, D., Pradas, M.M., Sanchez, M.S., 2009. Plasma Process. Polym. 6 (3), 190–198.
Garcia-Torres, J., Sylla, D., Molina, L., Crespo, E., Mota, J., Bautista, L., 2014. Appl. Surf. Sci. 305 (30), 292–300.
Guo, M., Chen, J., Liu, D., Nie, L., Yao, S., 2004. Bioelectrochemistry 62 (1), 29–35.
Guo, T., Zhao, X., Xie, X., Chen, Z., Zhou, C., Wei, L., Zhang, H., 2007. J. Int. Med. Res. 35 (3), 353–360.
He, T.T., Yang, Z.L., Chen, R., Wang, J., Leng, Y.X., Sun, H., Huang, N., 2012. Mater. Sci. Eng. C – Mater. Biol. Appl. 32 (5), 1025–1031.
Heineman, W.R., Wieck, H.J., Yacynych, A.M., 1980. Anal. Chem. 52 (2), 345–346.
Hirotsu, T., Tagaki, C., 2004. Thin Solid Films 457 (1), 20–25.
Hirotsu, T., Tagaki, C., Partridge, A., 2002. Plasmas Polym. 7 (4), 353–366.
Iwamoto, A., Mitsuda, K., Inoue, A., Kato, T., Inoue, Y., Kawahara, H., 2012. Cytotechnology 64 (3), 309–314.
Jeon, S.G., Yang, J.Y., Park, K.W., Kim, G.J., 2014. Bull. Korean Chem. Soc. 35 (12), 3583–3589.
Kaiser, H., 1973. Pure Appl. Chem. 34 (1), 35–62.
Kanehira, K., Banzai, T., Ogino, C., Shimizu, N., Kubota, Y., Sonezaki, S., 2008. Colloid. Surface. B. 64 (1), 10–15.
Kang, M., Wang, M., Zhang, S., Dong, X., He, L., Zhang, Y., Guo, D., Wang, P., Fang, S., Zhang, Z., 2015. Electrochim. Acta 161 (10), 186–194.
Keighley, S.D., Estrela, P., Li, P., Migliorato, P., 2008. Biosens. Bioelectron. 24 (4), 906–911.
Labib, M., Berezovski, M.V., 2014. Adv. Biochem. Eng. Biotechnol. 229 (10), 155–181.
Li, Y., Lei, C., Zeng, Y., Ji, X., Zhang, S., 2012. Chem. Commun. 48 (88), 10892–10894.
Liu, S., Yu, J., Jaroniec, M., 2010. J.A.C.S. 132 (34), 11914–11916.
Losic, D., Cole, M.A., Dollmann, B., Vasilev, K., Griesser, H.J., 2008. Nanotechnology 19 (24), 245704.
Mao, Y., Wei, W., Zhang, J., Zhang, S., Rao, X., 2001. Analyst 126 (9), 1568–1572.
Messina, G.M., Satriano, C., Marletta, G., 2009. Colloid. Surface. B 70 (1), 76–83.
Mihai, L., Vezeanu, A., Polonschii, C., Albu, C., Radu, G.L., Vasilescu, A., 2015. Sens. Actuat. B 206 (1), 198–204.
Nwankire, C.E., Venkatanarayanan, A., Glennon, T., Keyes, T.E., Forster, R.J., Ducrée, J., 2015. Biosens. Bioelectron. 68 (15), 382–389.
Pandiyaraj, K.N., Selvarajan, V., Rhee, Y.H., Kim, H.W., Pavese, M., 2010. Coll. Surf. B 79 (1), 53–60.
Pauliukaite, R., Ghica, M.E., Fatibello-Filho, O., Brett, C.M., 2010. Electrochim. Acta 55 (21), 6239–6247.
Peng, Y., Zhang, D., Li, Y., Qi, H., Gao, Q., Zhang, C., 2009. Biosens. Bioelectron. 25 (1), 94–99.
Pryce Lewis, H.G., Edell, D.J., Gleason, K.K., 2000. Chem. Mater. 12 (11), 3488–3494.
Ricciardi, S., Castagna, R., Severino, S.M., Ferrante, I., Frascella, F., Celasco, E., Mandracci, P., Vallini, I., Mantero, G., Pirri, C.F., 2012. Surf. Coat. Technol. 207 (25), 389–399.
Rivolo, P., Severino, S.M., Ricciardi, S., Frascella, F., Geobaldo, F., 2014. J. Colloid Interface Sci. 416 (15), 73–80.
Rodríguez, M.C., Rivas, G.A., 2009. Talanta 78 (1), 212–216.
Rohrbach, F., Karadeniz, H., Erdem, A., Famulok, M., Mayer, G., 2012. Anal. Biochem. 421 (2), 454–459.
Sciarratta, V., Vohrer, U., Hegemann, D., Müller, M., Oehr, C., 2003. Surf. Coat. Technol. 174 (11), 805–810.
Sener, G., Ozgur, E., Yılmaz, E., Uzun, L., Say, R., Denizli, A., 2010. Biosens. Bioelectron. 26 (2), 815–821.
Solís-Gómez, A., Neira-Velázquez, M.G., Morales, J., Sánchez-Castillo, M.A., Pérez, E., 2014. Coll. Surf. A 451 (1), 66–74.
Song, Y., Li, Y., Liu, Z.P., Liu, L.L., Wang, X.Y., Su, X.G., Ma, Q., 2014. Biosens. Bioelectron. 61 (15), 9–13.
Sundfors, F., Bobacka, J., Ivaska, A., Lewenstam, A., 2002. Electrochim. Acta 47 (13), 2245–2251.
Van Os, M., Menges, B., Förch, R., Knoll, W., Timmons, R., Vancso, G., 1998. MRS Proceedings. 544. Cambridge University Press, Cambridge, p. 45.
Venkatesh, A., Sun, A., Brickner, H., Looney, D., Hall, D.A., Aronoff-Spencer, E., 2015. Biosens. Bioelectron. 70 (15), 462–468.
Wang, J., 2005. Analyst 130 (4), 421–426.
Wang, J., Neoh, K., Kang, E., 2004. Thin Solid Films 446 (2), 205–217.
Wang, L., Li, L., Xu, Y., Cheng, G., He, P., Fang, Y., 2009. Talanta 79 (3), 557–561.
Wang, M., Zhai, S., Ye, Z., He, L., Peng, D., Feng, X., Yang, Y., Fang, S., Zhang, H., Zhang, Z., 2015. Dalton Trans. 44, 6473–6479.
Wang, X., Ju, J., Li, J., Li, J., Qian, Q., Mao, C., Shen, J., 2014. Electrochim. Acta 123 (20), 511–517.
Wang, Y., Pu, K.Y., Liu, B., 2010. Langmuir 26 (12), 10025–10030.
Ward, L., Schofield, W., Badyal, J., Goodwin, A., Merlin, P., 2003. Chem. Mater. 15 (7), 1466–1469.
Yang, M., Yang, Y., Yang, H., Shen, G., Yu, R., 2006. Biomaterials 27 (2), 246–255.
Zhang, Z., Chen, Q., Knoll, W., Foerch, R., Holcomb, R., Roitman, D., 2003. Macromolecules 36 (20), 7689–7694.
Zhang, Z., Liu, S., Shi, Y., Zhang, Y., Peacock, D., Yan, F., Wang, P., He, L., Feng, X., Fang, S., 2014a. J. Mater. Chem. B 2 (11), 1530–1538.